Materials Science and Engineering C 70 (2017) 223–230

Contents lists available at ScienceDirect

Materials Science and Engineering C

journal homepage: www.elsevier.com/locate/msec

Horseradish peroxidase and toluidine blue covalently immobilized leak-free sol-gel composite biosensor for hydrogen peroxide

K. Thenmozhi [a,*], S. Sriman Narayanan [b]

[a] Department of Chemistry, School of Advanced Sciences, VIT University, Vellore 632 014, India
[b] Department of Analytical Chemistry, University of Madras, Guindy Campus, Chennai 600 025, India

ARTICLE INFO

Article history:
Received 15 May 2016
Received in revised form 5 August 2016
Accepted 29 August 2016
Available online 31 August 2016

Keywords:
Horseradish peroxidase
Ceramic composite biosensor
Covalent immobilization
Cyclic voltammetry
Hydrogen peroxide

ABSTRACT

The enzyme horseradish peroxidase and the water-soluble mediator toluidine blue were covalently immobilized to 3-aminopropyl trimethoxy silane precursor through glutaraldehyde crosslinker. A rigid ceramic composite electrode was fabricated from this modified silane along with graphite powder, which resulted in an amperometric biosensor for H_2O_2. The electrochemical behaviour of the modified biosensor was monitored using cyclic voltammetry in the potential range of 0.2 V to −0.4 V vs SCE. The biosensor exhibited a stable voltammogram with cathodic peak at −0.234 V and anodic peak at −0.172 V, with a formal potential of −0.203 V. Various factors influencing the performance of the biosensor such as buffer solution, pH, temperature and potential were examined for optimizing the working conditions. The modified biosensor exhibited a good catalytic behaviour for the reduction of H_2O_2 at a lower potential of −0.25 V without any barrier from possible interferents. The analytical working range was found to be 0.429 μM to 0.455 mM of H_2O_2 with a detection limit of 0.171 μM. The fabricated biosensor is robust for long-term usage in addition to the high sensitivity, rapid response and having an advantage of surface renewability by simple mechanical polishing.

1. Introduction

Development of simple and reliable methods for the immobilization of enzymes is a crucial step in the fabrication of biosensors. The stability, reproducibility, sensitivity as well as lifetime of the biosensor depend on the strategy of immobilization of the enzymes. Immobilized enzymes are more robust and have the advantages of convenient handling, easy separation from the product, operational stability, more resistant to environmental changes and feasibility of reuse compared to free enzymes in solution. Many methods such as physical or chemical adsorption at a solid surface [1,2], incorporation into conducting polymers [3], bulk modified composites [4], and covalent immobilization [5], anchoring on arrays [6,7] or crosslinking to a matrix [8] have been used as valuable techniques for immobilization. But, the development of new strategies of immobilization is still an active field of research for enhancing the performance of the existing biosensors. The simplest method of biosensor fabrication is entrapment or adsorption of the biocatalyst (e.g. proteins, enzymes), which encounters several problems. In addition to the leaching of the biocatalysts, various factors hinders the direct electron transfer between the electrode and the enzymes or proteins, including slow electron transfer due to the deep burial of the electroactive cofactors in the proteins shell, denaturation of the protein at the electrode surface, and unfavorable orientation of the protein. To overcome these shortcomings, much effort has been focused on facilitating the electron transfer between proteins and electrodes, including the use of electron transfer mediators [9,10]. In the construction of mediated biosensors, immobilization of the mediator is also an important task as that of the enzyme [11]. The immobilization procedure should maintain the integrity and activity of the enzyme while utilizing mediators for enhancing the electron transfer rates.

Appropriate choice of mediator is crucial for added efficiency in electron transfer between the active site of the enzyme and the electrode surface. A variety of organic dyes have been used as electron shuttling agents, such as toluidine blue [12], thionine [13], brilliant green [14], methylene blue [15], methylene green [16], prussian blue [17], azure A [18] and phenazines [19]. All these dyes have been reported to have an excellent mediating ability in the bioelectrocatalytic reduction of H_2O_2. The problem associated with these low molecular weight dyes is their leachability from the electrode surface into the solution, which may lead to a significant signal loss and affects the performance of the biosensor. Hence efficient immobilization methods should be adopted while employing these mediators to enhance the performance of the biosensor [20].

Electrochemical methods surpass the defects of the conventional methods with attractive features of quick response, high sensitivity and abilities to be miniaturized [21–24]. Electrochemical enzyme based biosensors have gained marked attention as sensitive and

* Corresponding author.
E-mail address: kt.thenmozhi@gmail.com (K. Thenmozhi).

http://dx.doi.org/10.1016/j.msec.2016.08.075
0928-4931/

selective tool due to amplification of substrate turnover and the specificity of biological recognition unit [25–27]. Quantitation of H_2O_2 with reliable and accurate sensors is of great interest in many disciplines such as food, industrial and environmental monitoring, and particularly in biosensing since H_2O_2 is a by-product of several reactions catalysed by various oxidase enzymes. [28–34].

Sol-gel-derived materials have emerged with attractive features to incorporate all kinds of species [35–38]. These new kinds of inorganic materials are particularly attractive for electrochemical biosensor development, since they possess the advantages of both carbon based electrodes and sol-gel electrochemistry [39,40]. The smart features of sol-gel materials would further be enhanced by the use of bifunctional sol-gel precursors such as (3-aminopropyl) trimethoxy silane and (3-mercaptopropyl) trimethoxy silane which provide free amino groups and thiol groups that could be used as the binding site for covalent attachment of mediators and biomolecules [41,42]. These functional sol-gel precursors facilitate the construction of sensing materials with possible control over the selective modification, orientation and distribution of catalytic sites [43,44].

We report in this work for the first time, an efficient route for the covalent immobilization of both the enzyme and the mediator to the sol-gel matrix derived from 3-aminopropyl trimethoxy silane (APTMOS) and methyl trimethoxy silane (MTMOS) and develop a renewable amperometric biosensor for H_2O_2. In the ceramic composite composition, APTMOS provides the immobilization site for both the enzyme, Horseradish peroxidase (HRP) and the mediator, Toluidine blue (TB). The additional monomer, MTMOS serves to maintain the hydrophobicity/hydrophilicity of the composite. Here, graphite powder provides conductivity, APTMOS and MTMOS serves as binder and attribute to the rigidity and porosity, HRP acts as biocatalyst and TB for shutting electrons between the enzyme and the electrode surface. The enzyme composite electrode has been further applied for the determination of H_2O_2 in both static and dynamic conditions, after thorough optimization of the electrocatalytic performance.

2. Experimental

2.1. Reagents and solutions

HRP (RZ 3.0, 250 U mg^{-1}) was purchased from Sisco Research Laboratories and used as received. APTMOS, MTMOS and Graphite powder were obtained from Aldrich. Hydrogen peroxide (50%) was purchased from Merck. Toluidine blue was received from s.d. fine chemicals. All other chemicals were of reagent grade and used without further purification. Double distilled water was used for the preparation of solution and further dilutions. Electrochemical experiments were carried out in the background electrolyte of 0.05 M phosphate buffer. The solutions were purged with high purity N_2 for 15 min before commencing the experiments. The accurate concentration of H_2O_2 was determined by titration with $KMnO_4$.

2.2. Apparatus

The electrochemical experiments were performed in a conventional one-compartment cell with a three electrode configuration using a CHI 400 A Electrochemical Analyzer. The working electrode was HRP and TB modified ceramic composite biosensor (HRP/TB/CCB), the auxiliary electrode was a platinum wire and the saturated calomel electrode (SCE) served as the reference electrode. All the potentials measured and quoted in this paper are against SCE. Impedance measurements were performed in 2.0 mM $[Fe(CN)_6/]^{3/4-}$ with 0.1 M KCl as supporting electrolyte, within the frequency range of 100 kHz–1 Hz, using an alternating current voltage of 5 mV. A magnetic stirrer and a stirring bar provided the convective environment for the amperometric studies. An Elico pH meter (Model LI 120) was employed for pH measurements. FT-IR spectra were recorded on a PerkinElmer FTIR Spectrometer (Spectrum RX1) in KBr pellets.

2.3. Construction of HRP/TB/CCB

A mixture of 0.4 ml APTMOS, 0.6 ml MTMOS and 20 μl of 10 mM HCl were thoroughly shaken for 5 min. The composition of APTMOS/MTMOS was optimized to this value for maintaining the hydrophobicity/hydrophilicity of the composite. 30 mg of TB in 1 ml MeOH was allowed to stir with 40 μl glutaraldehyde (25%) for 30 min to permit the crosslinking of mediator with the linker.Separately, 0.5 ml of HRP solution (10 mg/ml in 0.05 M phosphate buffer; pH 7.00) was mixed with 40 μl of glutaraldehyde. Both the mediator and the enzyme linked glutaraldehyde solutions were sequentially added to the above sol-gel mixture and continued shaking for another 30 min. This would permit the unreacted aldehydic group of the glutaraldehyde to couple with the free amino groups of the sol-gel mixture.

Thereafter, 0.8 ml portion of this mediator and enzyme immobilized sol-gel mixture was added to 550 mg of graphite powder and blended totally and packed tightly into a glass vial (3 mm diameter). The tip was smoothened over weighing paper and used as working surface after allowing to dry at 4 °C in a refrigerator for 4 days. A copper wire inserted at the other end provided the electrical contact. Also, an unmodified ceramic composite electrode (CCE) was prepared in the absence of TB and HRP. Further a TB/CCE was prepared in the absence of HRP for comparative purposes.

3. Results and discussion

3.1. Covalent immobilization of TB and HRP

The use of glutaraldehyde as a cross-linker for covalent crosslinking of various reagents and enzymes possessing primary amino group through the formation of Schiff's base has been studied well [45]. In the present work, one of the terminal aldehyde group of the bifunctional cross-linker, glutaraldehyde condensed with amino group of HRP and TB by Schiff's base reaction separately as shown in the first step of the scheme. In the next step, the other free aldehyde group of these compounds was attached to primary amino groups (of APTMOS) in the sol-gel matrix by Schiff's base reaction to result in the covalent immobilization of sol-gel binder with TB and HRP. The steps involved in mediator and enzyme immobilization are illustrated in Scheme 1.

The covalent crosslinking of HRP and TB to APTMOS was confirmed by FTIR. Fig. 1 (curves a, b and c) represents the FTIR spectra of free TB, free HRP and sol-gel immobilized with TB and HRP. Fig. S1 represents the FT-IR spectrum of sol-gel matrix before the immobilization of TB and HRP showing the characteristics silane peaks. The spectrum of free TB shows (Fig. 1 (curve a)) two bands at 3380 cm^{-1} and 3145 cm^{-1} due to the N—H stretching vibration of the primary amino group which were not found in the spectrum of HRP/TB sol-gel matrix (Fig. 1 (curve c)). Also the sharp peak found at 1600 cm^{-1} corresponding to the N—H bending vibration of the free amino group was found to disappear in Fig. 1 (curve c) and a strong and broad band appeared at 1710 cm^{-1}. This might be due to the presence of imine groups due to the covalent immobilization of the TB (Fig. 1 (curve c)). In the spectrum of free HRP (Fig. 1 (curve b)) the band at 1695 cm^{-1} could be assigned to the C═O stretching mode of amide I and the absorption signal at 1595 cm^{-1} indicated a characteristic amide II band. The spectrum of sol-gel immobilized with both the mediator and the enzyme, shows the appearance of amide II band. The amide I band is expected to overlap with the signal of the imine groups. In Fig. 1 (curve c) the absorption at 3471 cm^{-1} may be due to the H-bonded silanol with water and the peaks at 1127 cm^{-1} and 1026 cm^{-1} showed the presence of Si—O—Si asymmetric stretching vibration [46]. The sharp band at 1277 cm^{-1} is assigned to Si-CH_3 symmetric deformation, and the absorption peak at 776 cm^{-1} may be due to the methyl rocking or Si—C stretching

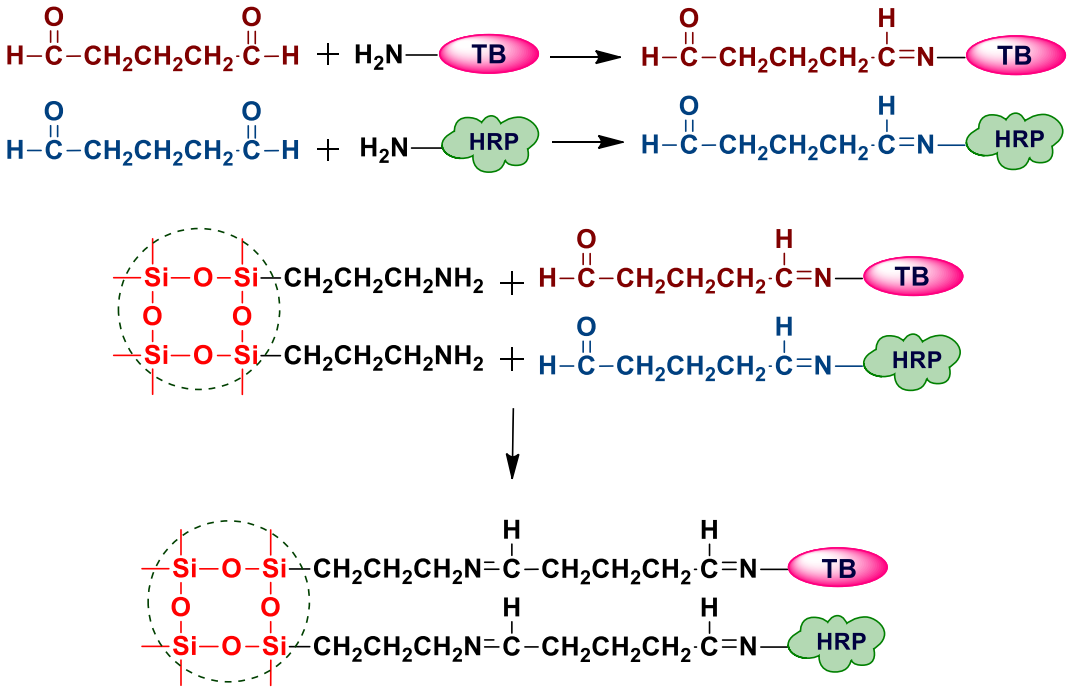

Scheme 1. Illustration of steps involved in the immobilization of TB and HRP to sol-gel matrix.

characteristic of the Si-CH_3 groups [47]. These results confirmed the covalent immobilization of TB and HRP in the sol-gel matrix and the immobilized HRP retained the essential features of its native secondary structure and its biological activity.

Electrochemical impedance spectroscopy (EIS) is a powerful tool to examine the interactions between the biomarkers and receptors indicated by the changes in the electrical impedance recorded. The charge transport behaviour of the electrode/electrolyte interface could be analysed extensively with EIS using a Nyquist plot. It is the plot of Z′ (Real component) versus Z″ (Imaginary component) representing the electron-transfer resistance with varying diameters on the semicircles. Fig. 2 represents the Nyquist plots recorded with bare CCE (curve a), TB/CCE (curve b) and HRP/TB/CCB (curve c) in a 0.1 M KCl containing 2 mM $[Fe(CN)_6]^{3/4-}$, at the formal potential of the redox couple. The electrolyte properties are represented by the area under higher frequency and the electrode/electrolyte interface properties are indicated by mid frequency region. Solution resistance (R_s) is given by the intercept of the curve with real axis and the charge transfer resistance (R_{ct}) of the electrode material is observed as depressed semicircle at higher frequencies [27]. A well-defined semicircle with R_{ct} of 548 Ω at higher frequency was obtained with bare CCE indicating the greater impedance at the interface. TB immobilization on the CCE decreased the charge transfer resistance to 238 Ω with lowest R_{ct} values and this shows that the conductivity is significantly improved in the presence of the mediator. With the HRP/TB/CCE the R_{ct} increased to 601 Ω which is

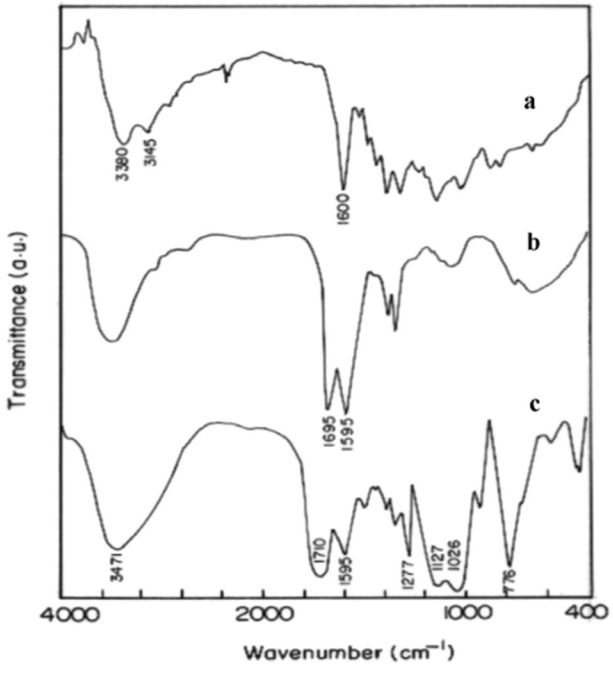

Fig. 1. FT-IR spectra of (a) Free Toluidine blue (b) Free Horseradish peroxidase (c) Sol-gel matrix immobilized with toluidine blue and horseradish peroxidase.

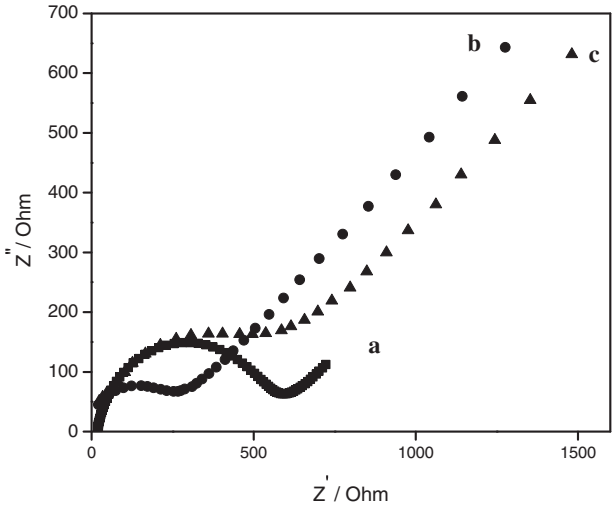

Fig. 2. Nyquist plots of (a) bare CCE, (b) TB/CCE, and (c) HRP/TB/CCB in 2.0 mM $[Fe(CN)_6]^{3/4-}$ with 0.1 M KCl as the supporting electrolyte. AC amplitude: 5 mV; frequency range: 100 kHz–1 Hz.

attributable to the attachment of the poorly conducing layer of HRP and consequent delay in electron-transfer from the bulkier enzyme moiety. These results conclude that the electron transfer resistance varied significantly during the immobilization process and finally an enhanced resistance was observed as a consequence of stable immobilization of HRP in the composite biosensor.

3.2. Electrochemical behaviour of HRP/TB/CCB

The electrochemical behaviors of the modified electrode HRP/TB/CCB and the blank electrode CCE were studied with cyclic voltammetry. Fig. 3 (curve c) shows the cyclic voltammetric response of the HRP/TB/CCB and the blank CCE (curve a) recorded in 0.05 M phosphate buffer (pH 7.00) in the potential range of 0.2 to −0.4 V. The voltammetric response of the modified electrode presented a couple of stable and well-defined redox peaks corresponding to toluidine blue with the reduction peak at −0.234 V and oxidation peak at −0.172 V. The formal potential ($E^{0'} = E_{pa} + E_{pc}/2$) calculated from the average of cathodic and anodic peak potentials was found to be −0.203 V. The peak separation ΔE_p, was found to be 62 mV at 20 mV s^{-1}. It can be observed that the formal potential of the immobilized mediator shifted from −0.210 V (Fig. S2) for free toluidine blue to −0.203 V due to the covalent crosslinking of the mediator to sol-gel matrix. No distinct peaks were observed at the bare CCE in the range studied. The cyclic voltammograms of the biosensor recorded at different scan rates of 5 to 250 mV s^{-1}, showed that both the cathodic and anodic peak currents increased linearly with square root of scan rate (Fig. 4). This observation was in accordance with a diffusion-controlled process occurring at the surface of the biosensor [48].

3.3. Electrocatalytic reduction of H_2O_2

The HRP/TB/CCB was applied for the determination of H_2O_2 to evaluate its analytical applicability. Fig. 3 presents the response of the blank CCE (curve a) and HRP/TB/CCB (curve c) in the absence and presence of

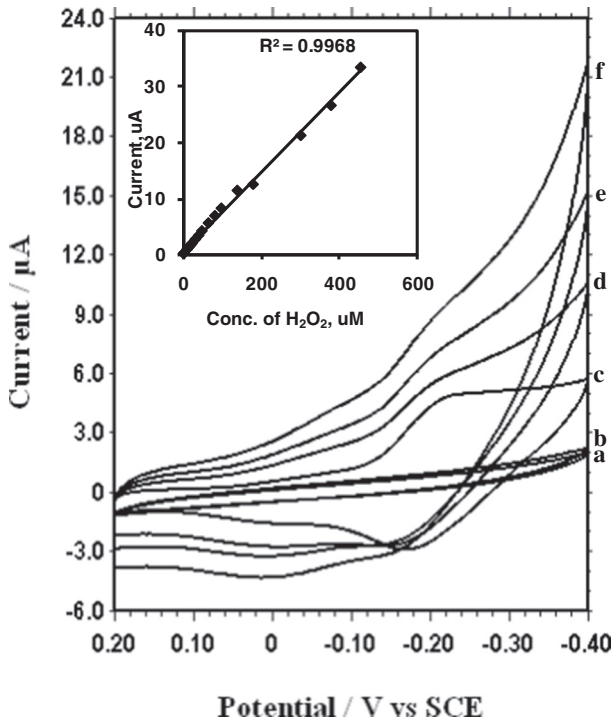

Fig. 3. Cyclic voltammograms of (a) bare CCE (b) 12 μM H_2O_2 at bare CCE (c) HRP/TB/CCB (d) 12 μM H_2O_2 (e) 29 μM H_2O_2 (f) 51 μM H_2O_2 at HRP/TB/CCB in 0.05 M phosphate buffer, pH 7.00; Scan rate: 20 mVs^{-1}. Inset: Calibration plot for the determination of Hydrogen peroxide.

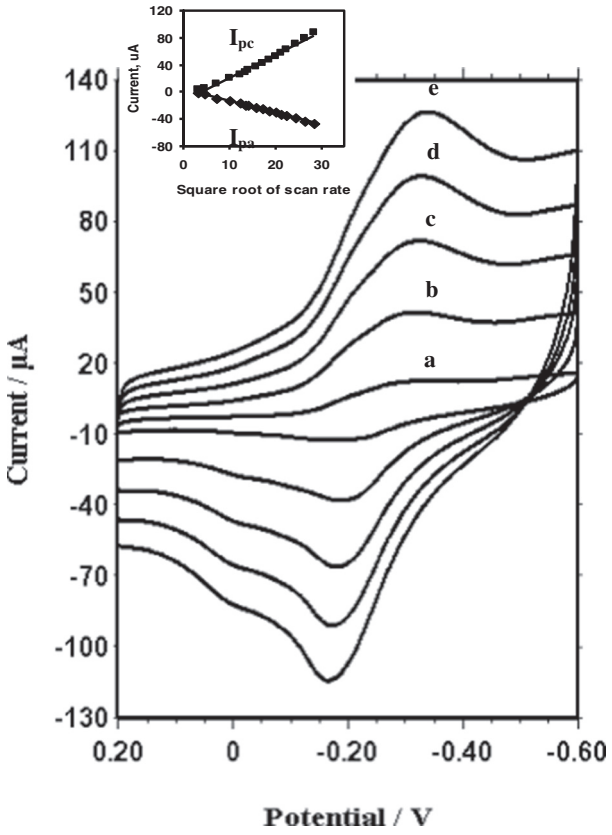

Fig. 4. Cyclic voltammograms of HRP/TB/CCB in 0.05 M Phosphate buffer at different scan rates: (a) 20 (b) 50 (c) 100 (d) 150 and (e) 200 mVs^{-1}. Inset: Variation of peak currents with square root of scan rates.

H_2O_2. The cyclic voltammetric studies showed that on every addition of H_2O_2, the cathodic peak current of HRP/TB/CCB increases drastically (Fig. 3 (curves d, e, f)). On the other hand, the blank CCE exhibited a feeble response at an elevated potential (curve b), showing that the direct reduction of H_2O_2 is hindered at the blank CCE. At the modified biosensor, the reduction of H_2O_2 occurs at a lower potential of −0.210 V with enhanced sensitivity. This demonstrates the mediator dependent electron transfer at the biosensor.

In the HRP catalysed reactions, the active site in HRP, a redox hemoglycoprotein is the sixth coordination position of Fe(III) in the Fe(III) protoporphyrin IX prosthetic group of the enzyme [49]. The HRP catalyses the reduction of H_2O_2 to water, during which the heme group of the active site of the enzyme (prosthetic group) gets oxidised to form an intermediate.

$$H_2O_2 + HRP \rightarrow H_2O + HRP\text{-}I \quad (1)$$

The oxidised heme group needs to be reduced to keep the activity and the oxidised enzyme is converted to its native form by the mediator through two separate one electron steps.

$$HRP\text{-}I + (TB)_{red} \rightarrow HRP\text{-}II + (TB)_{oxd} \quad (2)$$

$$HRP\text{-}II + (TB)_{red} \rightarrow HRP + (TB)_{oxd} \quad (3)$$

$$(TB)_{oxd} + 2e\text{-} \rightarrow (TB)_{red} \quad (4)$$

TB can then be regenerated electrochemically at the electrode leading to an increase in the reduction current, which indicated that TB incorporated in this matrix could effectively shuttle electrons between the electrode surface and the bioactive center of HRP. Thus, in the

presence of H_2O_2, the magnitude of current will be a function of the peroxide concentration. The efficiency of the biocatalytic reaction clearly depends on having all the steps in the sequence be rapid. It is generally accepted that steps (1) and (2) are indeed rapid and on the other hand step (3) can be sluggish requiring the use of an external redox mediator and hence TB was immobilized along with HRP to make this step also a fast one. Thus we adopted this design of mediated HRP biosensor for H_2O_2 determination and the representation of the biosensor function is shown as Scheme 2.

Quantification of H_2O_2 was carried out by recording the cyclic voltammograms of the HRP/TB/CCB in blank supporting electrolyte followed by successive addition of H_2O_2 aliquots. A calibration graph was constructed by plotting the catalytic current as a function of concentration of H_2O_2 (Inset to Fig. 3). The calibration plot for H_2O_2 was linear over the concentration range from 0.429 μM to 0.455 mM with a correlation coefficient of 0.9968. The detection limit has been calculated according to the formula $3\sigma/S$, where σ and S represent the blank standard deviation and sensitivity of determination respectively and was found to be 0.171 μM. The linear range for H_2O_2 determination and the detection limit obtained with the present sensor is greater than or comparable to that observed in the literature (Table 1). The high sensitivity of biosensor reflects the high efficiency of the immobilization strategy in which the activity of both the enzyme and the mediator are retained, which is a promising aspect for the development of amperometric biosensor.

The performance of the biosensor was optimized on various aspects of buffer, pH, temperature and potential. The effect of supporting electrolyte on the electrochemical behaviour of HRP/TB/CCB has been examined in different buffers in the presence of same concentration of H_2O_2 and at the same pH. In presence of 33.6 μM H_2O_2 at pH 7.00, highest sensitivity was recorded with phosphate buffer compared to HEPES and TRIS buffers. This behaviour may be assigned to the interaction between the phosphate and iron groups in the heme group of the enzyme and/or the facility of the phosphate ions to diffuse through the biosensor [56]. The effect of buffer concentration was also studied. Among 0.025 M, 0.05 M and 0.1 M phosphate buffers, best results were obtained with 0.05 M phosphate buffer, while others responded slightly different and hence 0.05 M phosphate buffer was chosen for the electrocatalytic studies.

The pH of the medium is an important parameter in determining the sensitivity of the enzyme catalysed reactions. The pH dependence of the system was studied over the range of pH 5 to 9 in the presence of 33.6 μM H_2O_2. The current response increased sharply on moving towards higher pH values and the maximum response was observed at pH 7. Beyond pH 7.5, the current response decreased (Fig. S3). The value of pH 7, where maximum response was observed was chosen as the operating pH value for further studies and this value was also in agreement with that of soluble peroxidase [57].

The thermal stability of HRP/TB/CCB was also studied by measuring the current response on varying the temperature of working solution from 20 to 60 °C in the presence of 33.6 μM H_2O_2. Temperature was an important variable which affected the amperometric response of the biosensor in two ways. The current increases rapidly from 20 to 40 °C, and then maintained a near similar response till 50 °C and decreased beyond that (Fig. S4). On one hand, there was an increase in sensitivity as a consequence of the dependence of the enzymatic activity upon temperature and on the other hand, degradation of the enzyme was accelerated with increasing temperature. Though the results presents a higher sensitivity at higher temperatures, to avoid the denaturation of the enzyme and to maintain the long term stability of the biosensor, the electrochemical measurements and electroanalysis were carried out at room temperature (25 °C).

3.4. Hydrodynamic voltammetry

To evaluate the operating potential for amperometric studies, hydrodynamic voltammograms were recorded in the potential range of 0.2 to −0.4 V. Fig. 5 shows the dependence of current response of both the modified biosensor and the blank CCE on the applied potential in the presence of 33.6 μM H_2O_2. It could be observed that the blank CCE showed a poor response even at higher potentials, while at the HRP/TB/CCB the response current increased sharply from 0 V and reached a near plateau beyond −0.25 V. Therefore a constant potential of −0.25 V was chosen as the working potential to minimize the possible interferences and to get the maximum response. The reduction of H_2O_2 is greatly enhanced at the biosensor compared to the blank as a result of bioelectrocatalysis.

3.5. Amperometry

The typical amperogram recorded for the successive additions of 1 ml of 34.4 μM H_2O_2 to a stirring supporting electrolyte solution of 0.05 M phosphate buffer (pH 7.00) at an operating potential of −0.25 V is shown in Fig. 6. Upon the addition of an aliquot of H_2O_2, the reduction current increases steeply to reach a stable value. The time required to reach 95% of the steady-state current was within 2 s reflecting the rapid and sensitive response of the biosensor towards H_2O_2. Such quick response is attributed to the high bioactivity of immobilized HRP as well as the speedy shuttling of electrons between the prosthetic groups of HRP and the electrode surface brought by the immobilized mediator. The thin wetting section controlled by the methyl groups of MTMOS also favours the quick response. Fig. 6 shows the part of amperometric measurements for H_2O_2 in the concentration range of 0.424 μM to 3.47 μM. The biosensor response is linear for H_2O_2 in the concentration range from 0.424 μM to 0.36 mM (Inset to Fig. 6).

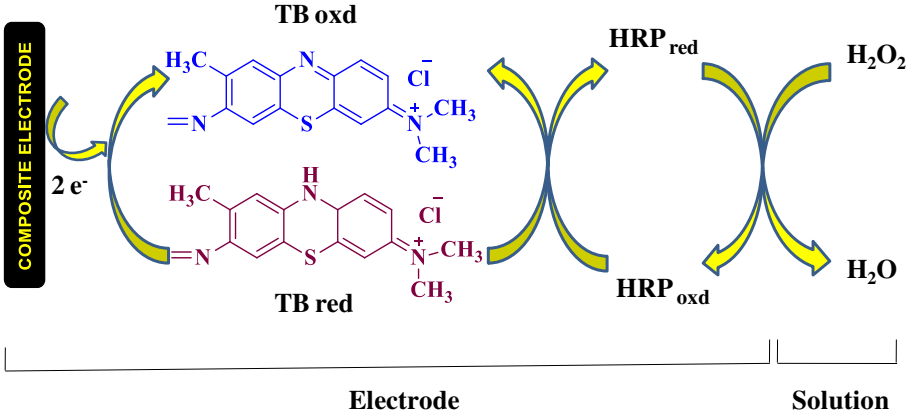

Scheme 2. Illustration showing the electrocatalytic reduction of H_2O_2.

Table 1
Comparison of the performance of various HRP biosensors.

Electrode	Potential	Linear range	LOD	Sensitivity	Response time (s)	Life time	Reference
PAN-PNMTh HRP electrode	−0.25 V vs SCE	5.0 μM–60.0 mM	3.2 μM	35 mA/M	2	87% after 30 days	[50]
HPC-Fc/HRP electrode	0.35 V vs Ag/AgCl	0.1 μM–8 μM	0.1 μM	4.21 nA/μM	–	90% after 2 weeks	[51]
HRP/TNW/ CPE	−0.38 V vs Ag/AgCl	0.25 mM–6.67 mM	1.2 μM	–	–	91% after 30 days	[52]
HRP/CMCS/ sol-gel	−0.4 V vs SCE	5 μM–1.4 mM	0.40 μM	0.624 mA/M	5	One month	[53]
TTP/SPCE	−0.1 vs Ag/AgCl	0.02–0.50 mM	4.10 μM	2.27 μA/mM	–	70% after 25 days	[54]
HRP-Nf-sonogel-biosensor	−0.25 vs Ag/AgCl	4 μM–100 μM	1.6 μM	12.8 nA/μM	35	91% after 15 days	[55]
HRP/TB/CCB	−0.25 V vs SCE	0.429 μM–0.455 mM	0.17 μM	0.071 μA/μM	2	86.7% after 3 months	Present work

3.6. Surface renewal repeatability and reproducibility

The composite biosensor is found to be attractive since both the enzyme and the mediator are immobilized throughout the bulk and only a thin section is wetted each time by the electrolyte. An inherent advantage of the biosensor designs based on rigid composite electrodes is their renewability by simple polishing [58]. Hence the biosensor can be renewed by a simple mechanical polishing step to get a full bioactive layer in event of surface fouling. The surface renewal reproducibility was tested on an electrode by measuring the current response in the presence of same concentration of 33.6 μM H_2O_2 after repeated surface polishings. Less than 3.6% R.S.D. was obtained during 10 polishes, demonstrating that fresh electrode surfaces were achieved by simple polishing. The measurement reproducibility of the same biosensor was examined towards 33.6 μM H_2O_2 for 8 successive recordings and the relative standard deviation was observed to be 2.9%. This shows that both the enzyme and the mediator have been uniformly immobilized and distributed throughout the body of the electrode.

3.7. Stability

The most remarkable factor about the biosensor is its stability, which was verified on several aspects. The operational stability was checked by monitoring the change in current response of the HRP/TB/CCB in the potential range of 0.2 to −0.4 V for continuous 100 cyclings. The electrode was proved to be appreciably stable with no observable decrease in current (Fig. 7).

The long-term stability of the sensor was followed by two different storage methods. One was stored at room temperature and another at 4 °C in a refrigerator under dry conditions. The performance of both the electrodes was tested in the presence of 33.6 μM H_2O_2 at regular intervals for 3 months. The biosensor stored at room temperature retained about 67% response and that stored at 4 °C exhibited 86.7% of its original sensitivity at the end of the study. The long-term operational stability of the biosensor for H_2O_2 determination is shown as Inset to Fig. 7. The working concentration range and response times were found to be reasonably consistent during this period. Also the regeneration ability allowed the biosensor to be used for the period of time of at least 90 days without any apparent loss of immobilized enzyme activity. In order to elucidate these results sufficiently, the biosensor was immersed in 0.05 M phosphate buffer solution for 24 h. On comparing the response of the biosensor before and after electrode immersion, it was found that the response remained constant, which meant that the biosensor remained substantially stable. By virtue of the robust nature of covalent immobilization of the enzyme and the mediator and the biologically favourable microenvironment for HRP, the biosensor exhibited remarkable stability.

3.8. Effect of interference

Interference study was carried out by comparing the current response before and after addition of some common and possible interferents occurring in biological, food and environmental samples. The effect of interfering species depends on the analyte chosen and the working potential. The interferents and H_2O_2 were taken in a ratio of 2:1 and the response studied. The current ratios were calculated by

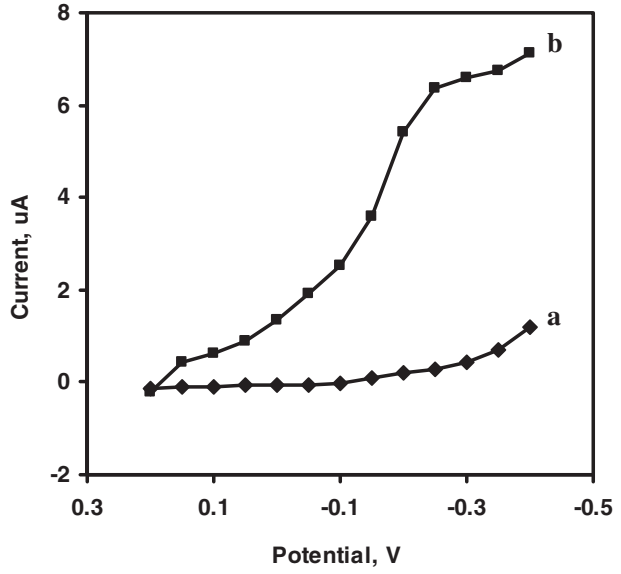

Fig. 5. Hydrodynamic voltammograms of 33.6 μM H_2O_2 at (a) HRP/TB/CCB and (b) blank CCE in 0.05 M phosphate buffer (pH 7.00); Stirring rate: 300 rpm.

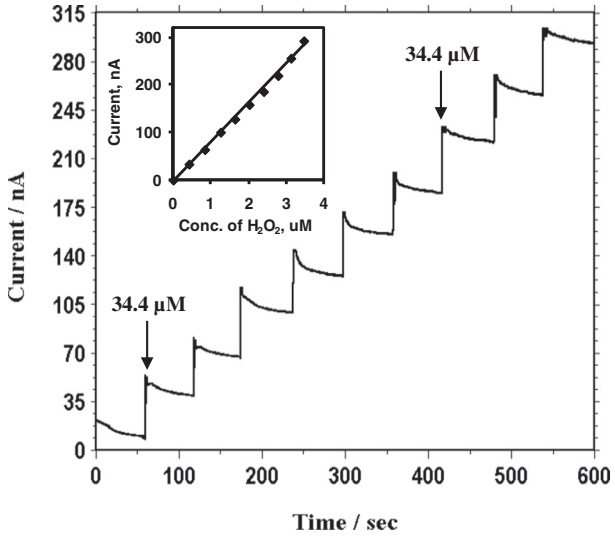

Fig. 6. Current-time response observed with HRP/TB/CCB for successive addition of 1 ml of 34.4 μM H_2O_2 in 0.05 M phosphate buffer (pH 7.00). Stirring rate: 300 rpm. Potential: −0.25 V. Inset: Calibration graph for H_2O_2 measurement.

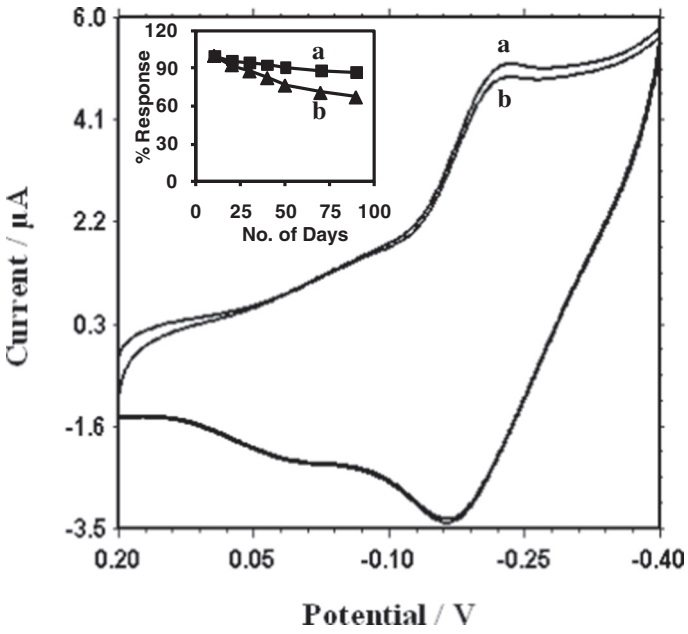

Fig. 7. Cyclic voltammograms of (a) 1st and (b) 100th scan of HRP/TB/CCB in 0.05 M Phosphate buffer, pH 7.0; Scan rate: 20 mVs^{-1}. Inset: Percentage response of HRP-TB-CCB towards 33.6 μM H_2O_2 over 90 days storage (a) at room temperature, (b) at 4 °C.

comparing the response current of the biosensor obtained in the test solution containing 33.6 μM H_2O_2 and 67.2 μM interferent with the response current obtained only in the presence of 33.6 μM H_2O_2. Most of the interferents like ascorbic acid, uric acid, acetaminophen, glucose, dopamine, citric acid, Ca^{2+}, K^+, Na^+, Cl^-, and CO_3^{2-} did not cause significant interference on the response of H_2O_2 biosensor except sulfide (Table S1). The reason for sulfide interference originates from that sulfide directly inhibits the activity of HRP [59]. While some interference from oxygen is expected, the voltammograms recorded were identical in aerated and deaerated solutions. The selectivity observed is due to the low working potential chosen, as a result of which interference from various electroactive species is minimized.

3.9. Real sample analysis

The application of the HRP/TB/CCB for the real sample analysis was done with milk samples, where H_2O_2 is often used as preservative. The analysis was carried out by spiking a known concentration of H_2O_2 in 0.05 M phosphate buffer (pH 7.00) containing 10% milk samples and recording their recoveries. The recovery of H_2O_2 was found in various milk samples of toned milk, double toned milk and pasteurized full cream milk. Prior to analysis, a blank was recorded without addition of H_2O_2 in milk sample solution, which showed no signal. Thus the biosensor showed high selectivity and registered good recoveries (98%) for real sample analysis (Table S2).

4. Conclusion

Renewable graphite-ceramic biosensor has been fabricated successfully based on the covalent immobilization of both the enzyme and the mediator to the sol-gel matrix via glutaraldehyde cross-linking method. The bifunctional sol-gel precursor APTMOS served as the immobilization host for covalently immobilizing HRP and TB producing a highly stable biosensor. The precise electrode preparation rendered a leak-free biosensor, otherwise would lead to loss of both enzyme and the mediator in the working environment. Furthermore, the biosensor catalytically reduced H_2O_2 at −0.25 V, which greatly reduced the overpotential. The rigid backbone resulting from sol-gel polymerization enables the generation of fresh active layer each time by simple mechanical polishing. The biosensor prepared as such showed higher operational and storage stability in combination with a higher sensitivity and wider linear range. The proposed biosensor has practically good anti-interferent ability due to the low operating potential. Further research in expanding the spectrum of possible practical application is underway.

Appendix A. Supplementary data

Supplementary data to this article can be found online at http://dx.doi.org/10.1016/j.msec.2016.08.075.

References

[1] Y. Haldorai, S.K. Hwang, A.I. Gopalan, Y.S. Huh, Y.K. Han, W. Voit, G.S. Anand, K.P. Lee, Direct electrochemistry of cytochrome *c* immobilized on titanium nitride/multi-walled carbon nanotube composite for amperometric nitrite biosensor, Biosens. Bioelectron. 79 (2016) 543–552.
[2] K. Kwak, S. Senthil Kumar, K. Pyo, D. Lee, Ionic liquid of a gold nanocluster: A versatile matrix for electrochemical biosensors, ACS Nano 8 (1) (2014) 671–679.
[3] M.M. Barsan, M.E. Ghica, C.M.A. Brett, Electrochemical sensors and biosensors based on redox polymer/carbon nanotube modified electrodes: A review, Anal. Chim. Acta 881 (2015) 1–23.
[4] J. Wang, M. Musameh, Carbon nanotube/teflon composite electrochemical sensors and biosensors, Anal. Chem. 75 (9) (2003) 2075–2079.
[5] S. Cosnier, Biomolecule immobilization on electrode surfaces by entrapment or attachment to electrochemically polymerized films. A review, Biosens. Bioelectron. 14 (1999) 443–456.
[6] S.A. Skoog, P.R. Miller, R.D. Boehm, A.V. Sumant, R. Polsky, R.J. Narayan, Nitrogen-incorporated ultrananocrystalline diamond microneedle arrays for electrochemical biosensing, Diam. Relat. Mater. 54 (2015) 39–46.
[7] P.R. Miller, R.J. Narayan, R. Polsky, Microneedle based sensors for biodiagnosis, J. Mater. Chem. B 4 (2016) 1379–1383.
[8] P. Pinyou, A. Ruff, S. Pöller, S. Alsaoub, S. Leimkühler, U. Wollenberger, W. Schuhmann, Wiring of the aldehyde oxidoreductase PaoABC to electrode surfaces via entrapment in low potential phenothiazine-modified redox polymers, Bioelectrochemistry 109 (2016) 24–30.
[9] S.S. Razola, E. Aktas, J.C. Viré, J.-M. Kauffmann, Reagentless enzyme electrode based on phenothiazine mediation of horseradish peroxidase for subnanomolar hydrogen peroxide determination, Analyst 125 (2000) 79–85.
[10] M. Karadag, C. Geyik, D.O. Demirkol, F.N. Ertas, S. Timur, Modified gold surfaces by 6-(ferrocenyl)hexanethiol/dendrimer/gold nanoparticles as a platform for the mediated biosensing applications, Mater. Sci. Eng. C 33 (2013) 634–640.
[11] A. Chaubey, B.D. Malhotra, Mediated biosensors, Biosens. Bioelectron. 17 (2002) 441–456.
[12] K. Thenmozhi, S. Sriman Narayanan, Electrocatalytic reduction of nitrite ion on a toluidine blue sol-gel thin film electrode derived from 3-aminopropyl trimethoxy silane, Electroanalysis 19 (22) (2007) 2362–2368.

[13] T. Wang, R. Zhu, J. Zhuo, Z. Zhu, Y. Shao, M. Li, Direct detection of DNA below ppb level based on thionin functionalized layered MoS_2 electrochemical sensors, Anal. Chem. 86 (24) (2014) 12064–12069.
[14] M.E. Ghica, C.M.A. Brett, Poly(brilliant green) and poly(thionine) modified carbon nanotube coated carbon film electrodes for glucose and uric acid biosensors, Talanta 130 (2014) 198–206.
[15] M. Arvand, S. Sohrabnezhad, M.F. Mousavi, M. Shamsipur, M.A. Zanjanchi, Electrochemical study of methylene blue incorporated into mordenite type zeolite and its application for amperometric determination of ascorbic acid in real samples, Anal. Chim. Acta 491 (2) (2003) 193–201.
[16] Z. Wang, M. Etienne, V. Urbanova, G.W. Kohring, A. Walcarius, Reagentless D-sorbitol biosensor based on D-sorbitol dehydrogenase immobilized in a sol-gel carbon nanotubes-poly(methylene green) composite, Anal. Bioanal. Chem. 405 (11) (2013) 3899–3906.
[17] M. Orellana, P. Arriola, R.D. Río, R. Schrebler, R. Cordova, F. Scholz, H. Kahlert, Chronocoulometric study of the electrochemistry of Prussian blue, J. Phys. Chem. B 109 (32) (2005) 15483–15488.
[18] C.G. Anquela, T. García-Mendiola, J.M. Abad, M. Pita, F. Pariente, E. Lorenzo, Scaffold electrodes based on thioctic acid-capped gold nanoparticles coordinated alcohol dehydrogenase and azure a films for high performance biosensor, Bioelectrochemistry 106 (2015) 335–342.
[19] C.A. Pessoa, Y. Gushikem, L.T. Kubota, L. Gorton, Preliminary electrochemical study of phenothiazines and phenoxazines immobilized on zirconium phosphate, J. Electroanal. Chem. 431 (1) (1997) 23–27.
[20] F. Scholz, U. Schröder, R. Gulaboski, A. Doménech-Carbó, Electrodes with Immobilized Particles and Droplets: Three-phase Electrodes, 2nd edition Springer International Publishing, Switzerland, 2015 182, http://dx.doi.org/10.1007/978-3-319-10843-8_2.
[21] M. Baghayeri, A. Amiri, S. Farhadi, Development of non-enzymatic glucose sensor based on efficient loading Ag nanoparticles on functionalized carbon nanotubes, Sensors Actuators B Chem. 225 (2016) 354–362.
[22] M. Baghayeri, M. Namadchian, H. Karimi-Maleh, H. Beitollahi, Determination of nifedipine using nanostructured electrochemical sensor based on simple synthesis of Ag nanoparticles at the surface of glassy carbon electrode: Application to the analysis of some real samples, J. Electroanal. Chem. 697 (2013) 53–59.
[23] M. Baghayeri, B. Maleki, R. Zarghani, Voltammetric behavior of tiopronin on carbon paste electrode modified with nanocrystalline Fe50Ni50 alloys, Mater. Sci. Eng. C 44 (2014) 175–182.
[24] M. Baghayeri, M.B. Tehrani, A. Amiri, B. Maleki, S. Farhadi, A novel way for detection of antiparkinsonism drug entacapone via electrodeposition of silver nanoparticles/functionalized multi-walled carbon nanotubes as an amperometric sensor, Mater. Sci. Eng. C 66 (2016) 77–83.
[25] M. Baghayeri, M. Namadchian, Fabrication of a nanostructured luteolin biosensor for simultaneous determination of levodopa in the presence of acetaminophen and tyramine: Application to the analysis of some real samples, Electrochim. Acta 108 (2013) 22–31.
[26] M. Baghayeri, Glucose sensing by a glassy carbon electrode modified with glucose oxidase and a magnetic polymeric nanocomposite, RSC Adv. 5 (2015) 18267–18274.
[27] M. Baghayeri, H. Veisi, H. Veisi, B. Maleki, H. KarimiMaleh, H. Beitollahi, Multi-walled carbon nanotubes decorated with palladium nanoparticles as a novel platform for electrocatalytic sensing applications, RSC Adv. 4 (2014) 49595–49604.
[28] M. Baghayeri, E.N. Zare, M.M. Lakouraj, A simple hydrogen peroxide biosensor based on a novel electro-magnetic poly(p-phenylenediamine)@Fe_3O_4 nanocomposite, Biosens. Bioelectron. 55 (2014) 259–265.
[29] M. Baghayeri, H. Veisi, Fabrication of a facile electrochemical biosensor for hydrogen peroxide using efficient catalysis of hemoglobin on the porous Pd@Fe_3O_4-MWCNT nanocomposite, Biosens. Bioelectron. 74 (2015) 190–198.
[30] M. Baghayeri, E.N. Zare, M.M. Lakouraj, Monitoring of hydrogen peroxide using a glassy carbon electrode modified with hemoglobin and a polypyrrole-based nanocomposite, Microchim. Acta 182 (2015) 771–779.
[31] M. Baghayeri, E.N. Zare, M. Namadchian, Direct electrochemistry and electrocatalysis of hemoglobin immobilized on biocompatible poly(styrene-alternative-maleic acid)/functionalized multi-wall carbon nanotubes blends, Sensors Actuators B Chem. 188 (2013) 227–234.
[32] M. Baghayeri, E.N. Zare, R. Hasanzadeh, Facile synthesis of PSMA-g-3ABA/MWCNTs nanocomposite as a substrate for hemoglobin immobilization: Application to catalysis of H_2O_2, Mater. Sci. Eng. C 39 (2014) 213–220.
[33] M. Baghayeri, E.N. Zare, M.M. Lakouraj, Novel superparamagnetic PFu@Fe_3O_4 conductive nanocomposite as a suitable host for hemoglobin immobilization, Sensors Actuators B Chem. 202 (2014) 1200–1208.
[34] P. Rahimi, H.A. Rafiee-Pour, H. Ghourchian, P. Norouzi, M.R. Ganjali, Ionic-liquid/NH_2-MWCNTs as a highly sensitive nano-composite for catalase direct electrochemistry, Biosens. Bioelectron. 25 (2010) 1301–1306.
[35] O. Lev, Diagnostic applications of organically doped sol-gel porous-glass, Analusis 20 (9) (1992) 543–553.
[36] J. Wang, P.V.A. Pamidi, D.S. Park, Screen-printable sol-gel enzyme-containing carbon inks, Anal. Chem. 68 (15) (1996) 2705–2708.
[37] A.A. Ensafi, M. Jafari-Asl, B. Rezaei, M.M. Abarghoui, H. Farrokhpour, Facile synthesis of Pt-Pd@silicon nanostructure as an advanced electrocatalyst for direct methanol fuel cells, J. Power Sources 282 (2015) 452–461.
[38] S. Senthil Kumar, K. Kwak, D. Lee, Electrochemical sensing using quantum-sized gold nanoparticles, Anal. Chem. 83 (9) (2011) 3244–3247.
[39] T.M. Park, E.I. Iwuoha, M.R. Smyth, R. Freaney, A.J. McShane, Sol-gel based amperometric biosensor incorporating an osmium redox polymer as mediator for detection of L-lactate, Talanta 44 (6) (1997) 973–978.
[40] K. Thenmozhi, S. Sriman Narayanan, Surface renewable sol-gel composite electrode derived from 3-aminopropyltrimethoxy silane with covalently immobilized thionin, Biosens. Bioelectron. 23 (2007) 606–612.
[41] D. Ravi Shankaran, N. Uehera, T. Kato, Determination of hydrogen peroxide based on a metal dispersed sol-gel derived ceramic-graphite composite electrode, Anal. Bioanal. Chem. 374 (3) (2002) 412–415.
[42] S. Dehdashtiana, M.B. Gholivand, M. Shamsipur, Z. Karimi, A nano sized functionalized mesoporous silica modified carbon paste electrode as a novel, simple, robust and selective anti-diabetic metformin sensor, Sensors Actuators B Chem. 221 (2015) 807–815.
[43] W. Jin, J.D. Brennan, Properties and applications of proteins encapsulated within sol-gel derived materials, Anal. Chim. Acta 461 (1) (2002) 1–36.
[44] Y. Shen, T. Wu, Y. Zhang, J. Li, Comparison of two-typed (3-mercaptopropyl)trimethoxysilane-based networks on Au substrates, Talanta 65 (2) (2005) 481–488.
[45] E. Katz, D.D. Schlereth, H.L. Schmidt, A.J. Olsthoorn, Reconstitution of the quinoprotein glucose-dehydrogenase from its apoenzyme on a gold electrode surface-modified with a monolayer of pyrroloquinoline quinine, J. Electroanal. Chem. 368 (1–2) (1994) 165–171.
[46] R. Liang, J. Qui, P. Cai, A novel amperometric immunosensor based on three-dimensional sol-gel network and nanoparticle self-assemble technique, Anal. Chim. Acta 534 (2) (2005) 223–229.
[47] P. Taranekar, X. Fan, R. Advincula, Distinct surface morphologies of electropolymerized polymethylsiloxane network polypyrrole and comonomer films, Langmuir 18 (2002) 7943–7952.
[48] F.D. Munteanu, Y. Okamoto, L. Gorton, Electrochemical and catalytic investigation of carbon paste modified with toluidine blue O covalently immobilised on silica gel, Anal. Chim. Acta 476 (1) (2003) 43–54.
[49] H.B. Dunford, J. Everse, K. Everse, M. Grisham (Eds.), Peroxidases in Chemistry and Biology, 2, CRC Press, New York 1991, pp. 1–24.
[50] C. Chen, X. Hong, T. Xu, A. Chen, L. Lu, Y. Gao, Hydrogen peroxide biosensor based on the immobilization of horseradish peroxidase onto a poly(aniline-*co*-*N*-methylthionine) film, Synth. Met. 212 (2016) 123–130.
[51] P. Li, H. Kanga, C. Zhang, W. Li, Y. Huang, R. Liu, Reversible redox activity of ferrocene functionalized hydroxypropyl cellulose and its application to detect H_2O_2, Carbohydr. Polym. 140 (2016) 35–42.
[52] J.V. Nicolini, H.C. Ferraz, N. Solange de Resende, Immobilization of horseradish peroxidase on titanate nanowires for biosensing application, J. Appl. Electrochem. 46 (1) (2016) 17–25.
[53] Q. Xu, C. Mao, N.N. Liu, J.J. Zhu, J. Sheng, Direct electrochemistry of horseradish peroxidase based on biocompatible carboxymethyl chitosan-gold nanoparticle nanocomposite, Biosens. Bioelectron. 22 (5) (2006) 768–773.
[54] N.C. Sekar, L. Ge, S.A.M. Shaegh, S.H. Ng, S.N. Tan, A mediated turnip tissue paper-based amperometric hydrogen peroxide biosensor, Sensors Actuators B Chem. 210 (2015) 336–342.
[55] M. ElKaoutit, I. Naranjo-Rodriguez, M. Domınguez, M.P. Hernandez-Artigá, D. Bellido-Milla, J.L.H.-H. de Cisneros, A third-generation hydrogen peroxide biosensor based on horseradish peroxidase (HRP) enzyme immobilized in a nafion–nonogel–carbon composite, Electrochim. Acta 53 (24) (2008) 7131–7137.
[56] S.S. Rosatto, L.T. Kubota, G.O. Neto, Biosensor for phenol based on the direct electron transfer blocking of peroxidase immobilising on silica-titanium, Anal. Chim. Acta 390 (1–3) (1999) 65–72.
[57] A.C. Maehly, Plant Peroxidases: Methods in Enzymology, 11, Academic Press, New York, 1995 807.
[58] B. Serra, B. Benito, L. Agui, A.J. Reviejo, J.M. Pingarron, Graphite-teflon-peroxidase composite electrochemical biosensors. A tool for the wide detection of phenolic compounds, Electroanalysis 13 (8–9) (2001) 693–700.
[59] S.L. Chut, J. Li, S.N. Tan, Reagentless amperometric determination of hydrogen peroxide by silica sol-gel modified biosensor, Analyst 122 (11) (1997) 1431–1434.